International Journal of Fracture **69:** 357–369, 1995.

Initiation of parallel cracks from surface of elastic half-plane

YUAN N. LI, ANN P. HONG and ZDENĚK P. BAŽANT*
Department of Civil Engineering, Northwestern University, Evanston, Illinois 60208, USA

Received 18 January 1994; accepted 30 October 1994

Abstract. The paper deals with the problem of initiation of thermal or shrinkage cracks from the surface of a half plane. Linear elastic fracture behavior is assumed. The initial spacing and initial stable equilibrium length of parallel equidistant cracks emanating from the surface is determined from three conditions formulated in a preceding study of penetration of sea ice plate: (1) The stress at the surface reaches a given strength limit. (2) After the initial cracks form, the energy release rate equals its given critical value. (3) The finite energy release due to the initial crack jump equals the energy needed to form the crack (according to the given fracture energy of the material or fracture toughness). The problem is reduced to a singular integral equation which is solved numerically by Erdogan's method. The results of analysis appear to be compatible with the experimental evidence on thermal cracking in glass, and appear to give also reasonable predictions for thermal cracking on top of sea ice plates and shrinkage cracking in concrete.

1. Introduction

In the field of fracture mechanics, attention is usually focused on the problem of how cracks develop in structures that already have them. All brittle materials, of course, contain microcracks to begin with. However, these microcracks cannot be taken into account on the basis of linear elastic fracture mechanics because the critical fracture energy for the microcracks is different from that for the macrocracks, which are of interest here. The effect of the microcracks is embedded in the value of the strength limit of the material. The linear elastic fracture mechanics contains only one material failure characteristic – the fracture energy (or fracture toughness) of the material, and because the stress intensity factor for the limit of a zero crack length is zero, the initial macroscopic cracks cannot be described by the theory. To remedy, linear elastic fracture mechanics must obviously be supplemented by strength criterion.

Formation of initial macroscopic cracks from a smooth surface is important for many applications. For instance, in large blocks of concrete, large periodic cracks can appear suddenly due to drying. In the case of reinforced concrete beams, cracks of a certain spacing form at the tensile face when the applied load becomes large enough [6]. In drying lake beds and mud flats, cracks with a honeycomb pattern emerge after some period of drying. Similar cracks, whose observations allow geologists to deduce some characteristics of volcanic process, appear in cooling lava flows [10]. When a floating sea ice plate is subjected to a vertical load, star-shaped cracks of finite length radiate suddenly from the loaded area when the applied load reaches a certain level. Spacing of thermal cracks produced in hot rock by circulation of cold water is important for the hot dry rock geothermal energy scheme [4]. In all these situations, cracks of macroscopic sizes form at a smooth surface. Since there is no initial crack

* Walter P. Murphy Professor of Civil Engineering.

or notch at the surface, these problems cannot be analyzed by a straightforward application of the linear elastic fracture mechanics.

The phenomena of crack formation are often complicated by the randomness of material inhomogeneity. The initial cracks rarely appear in a regular and systematic way. In the case of large concrete blocks, the cracks are never straight and the spacing between these cracks is hardly uniform. In the case of a drying lake bed, the crack pattern is not exactly hexagonal and includes also pentagons and heptagons. However, the hexagon is the most common shape, and the sizes of these hexagons are almost uniform. In the case of penetration of a sea ice plate, it is found that the total number of radial cracks varies from experiment to experiment, but generally larger punch sizes produce more radial cracks [7]. Despite the randomness, there must nevertheless be deterministic laws governing the mean behavior. We will rigorously analyze the idealized two-dimensional problem of cooling of a perfectly homogeneous half-plane, in which we expect the initial cracks to be straight and their spacing and length, uniform.

Li and Bažant [11] discussed the problem of crack initiation for the case of vertical penetration of a floating sea ice plate. Since the penetration load depends on the number of radial cracks, it is essential to understand how the number of cracks is determined. Three basic conditions governing the penetration of the initial cracks in the ice penetration problem were proposed. In this paper, these three conditions, which involve the consideration of strength, will be applied to study the initiation of parallel cracks from the surface of an elastic half-plane under the action of initial strains. The initial strains can be caused by a drop of temperature or by drying shrinkage of the material. Because the nature of the applied loads as well as the geometry differ from the sea ice penetration problem, the theory will need to be restated and modified. The analysis will reveal some interesting new features of the crack initiation problem. The solution will be applied to the cooling cracks in glass, cooling cracks on top of a floating sea ice plate, and drying shrinkage cracks in concrete.

2. Conditions governing crack initiation from smooth surface

The phenomenon of crack initiation involves transition between two states: One is the initial equilibrium state in which there are no cracks. The other is the first state of stable equilibrium at which the cracks have formed and have come to a stop but are simultaneously in a critical condition from which they can propagate further in a stable equilibrium manner if the applied load is increased. Between these two states, the cracks are unstable and grow dynamically. The reason that the transition is dynamic is that the energy release rate as a function of crack length begins increasing from zero, while at the same time the energy consumption rate is constant and nonzero (because we are treating the problem according to linear elastic fracture mechanics, supplemented by the strength criterion). This is what causes the initial instability of crack growth. In this study we are interested only in the two equilibrium states and the basic laws governing them. Because the material is considered to be elastic, the response is path independent, and so the dynamic transition between these two states need not be analyzed in order to solve the crack spacing problem.

The first condition governing the crack initiation is a stress condition: The tensile stress caused by cooling or drying before the cracking must reach the tensile strength of the material at least at one point. For any load below this level the material simply can not start to break.

The second condition is that the final state, as we have defined it, satisfies the Griffith law, that is, the energy release rate must be equal to its critical value (called fracture energy). If

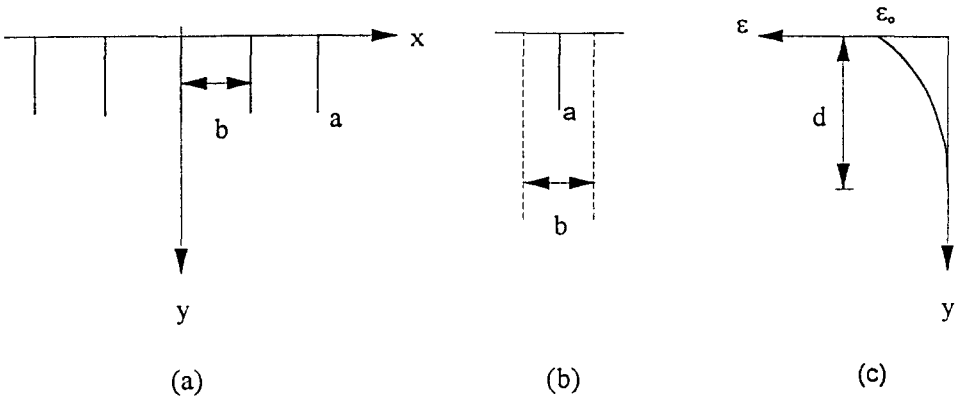

Fig. 1. (a) Geometry definition of crack systems; (b) Unit strip of width b; (c) Initial strain profile.

the energy release rate were above the critical value, then the cracks already formed would be unstable and would not stop at the final state. On the other hand, if the energy release rate were below the critical value, then the cracks would have had to stop earlier and that state would not represent the final state of the initial dynamic process.

The third condition is provided by the law of energy conservation, which requires the potential energy of the structure released due to crack jump to be fully converted into the surface energy of the newly formed cracks. Note that the Griffith law (the second condition) is also a statement of energy which is however applied to an infinitesimal crack extension and is represented by a differentiation of the potential energy, whereas the third condition is an energy conservation condition for a finite crack jump and is expressed by a finite difference in potential energy.

Consider now an elastic half-plane of unit thickness that occupies the region $y \geqslant 0$ (Fig. 1a) and is under plane stress. The material is homogeneous and isotropic. The half-plane is subjected to initial strain $\varepsilon_x = \varepsilon_0 f(y/d)$ which may be caused by cooling or drying of the surface; f is a given function and d is the penetration depth of cooling or drying. The initial stress is $\sigma_x = E\varepsilon_x = \varepsilon_0 E f(y/d)$. The general shape of function $f(y/d)$ is shown in Fig. 1c and its precise definition will be given later. We assume that the initially formed cracks are of equal length a and have a uniform spacing b. Thus we may concentrate on one cell of width b as shown in Fig. 1b. The three conditions of crack initiation can simply be written as

$$\sigma_x(x,0) \geqslant f_t; \quad G(a,d;b) = G_f; \quad U(0,d;b) - U(a,d;b) = aG_f, \tag{1}$$

where within the cell of width b, U = strain energy, f_t = tensile strength of the material; G_f = fracture energy of the material. For simplicity, we use here for the stress condition the equality $\sigma_x = f_t$, and postpone consideration of the case of inequality. In the following derivation, we will make use of Irwin's formula for the energy release rate in terms of the stress intensity factor

$$G = -\frac{\mathrm{d}U}{\mathrm{d}a} = \frac{K^2}{E}, \tag{2}$$

where K = mode I stress intensity factor at the crack tip and E = Young's modulus of the elastic material. With this relation and based on the third condition, we can express the strain energy change as

$$U(0,d;b) - U(a,d;b) = \frac{1}{E}\int_0^a K^2\,\mathrm{d}a. \tag{3}$$

Furthermore, by combining the second and third conditions and rearranging, we can cast the three basic conditions as:

$$\sigma_x = f_t; \quad K^2 = EG_f; \quad aK^2 = \int_0^a K^2\,\mathrm{d}a. \tag{4}$$

Since all the equations refer only to a unit cell of width b (which is equal to crack spacing), the second condition of crack initiation furnishes a relation between the ratios a/b and d/b. In this way, the solution of the crack initiation problem yields K as a function of a/b and d/b for the given initial strain profile. In other words, there is a one-to-one correspondence between crack spacing b and the loading depth d. Once the penetration depth d is given, the crack spacing b and the initial crack length a can also be determined. We will come back to this point later.

3. Mathematical formulation and numerical method

Since all these quantities are complicated functions of the geometrical configuration and the loading profile, the solution must be numerical. The following method can be used.

The problem is first decomposed into two separate problems. The first is the structure without cracks with the initial (or residual) stresses applied. The second is the structure without initial stress, but with cracks and crack surface tractions that are equal in magnitude to the initial stresses but opposite in direction. The solution is obtained by the superposition of these two problems. Since there is no stress intensity factor in the first problem, we can, therefore, study only the second problem. The initial strain profile may be considered either an error function (which is the exact solution of the linear diffusion problem) or a parabolic function (which is an often used approximation). These functions are

$$f(y) = 1 - \frac{2}{\sqrt{\pi}}\int^{\sqrt{3}y} e^{-u^2}\,\mathrm{d}u \quad \text{or} \quad f(y) = (1-y)^2, \quad 0 \leqslant y \leqslant 1. \tag{5}$$

The problem of a half space weakened by equidistant parallel surface cracks has been studied by Bažant, Ohtsubo and Aoh [3][5] using the finite element method, by Nemat-Nasser, Keer and Parihar [12] using numerical solution of integral equation based on the continuous dislocation representation of cracks, and by Nied [14] using the displacement jump as the basic unknown. The problem was also reviewed in Bažant and Cedolin's book [2] (Chapter 12). The stresses for one normal surface crack in a half space were given by Keer and Chantaramungkorn [9]. Nemat-Nasser, Keer and Parihar [12] modified their expression to obtain the stresses for an array of equidistant cracks at the surface. When all the cracks are of equal length, as assumed here, the equation can be simplified. The condition that the stress at the surface would reach the tensile strength may be written as

$$\sigma_x(0,y) = \int_0^a D(t)\sum_{n=-\infty}^{\infty} g(t,nb,y)\,\mathrm{d}t = -f(y/d), \tag{6}$$

where $D(t)$ is the density function of the Burger's vectors of edge dislocation multiplied by $E/4\pi$. The kernel function g can be expressed as

$$g(t,x,y) = \frac{2(y+t)}{(y+t)^2+x^2} - \frac{(y+3t)[(y+t)^2-x^2]}{[(y+t)^2+x^2]^2} + \frac{4ty(y+t)[(y+t)^2-3x^2]}{[(y+t)^2+x^2]^3} - \frac{(y-t)[(y-t)^2+3x^2]}{[(y-t)^2+x^2]^2}. \tag{7}$$

Since g is an even function of x, the series in (6) may be written as

$$\sum_{n=-\infty}^{\infty} g(t,nb,y) = g(t,0,y) + 2\sum_{n=1}^{\infty} g(t,nb,y). \tag{8}$$

Using the following two formulae (by Gradshteyn and Ryzhik, [8] pp. 23 and 36)

$$\sum_{n=1}^{\infty} \frac{1}{x^2+n^2} = \frac{1}{2x^2}[\pi x \coth \pi x - 1], \tag{9}$$

$$\sum_{n=1}^{\infty} \frac{x^2-n^2}{(x^2+n^2)^2} = \frac{\pi^2}{2}\operatorname{csch}^2 \pi x - \frac{1}{2x^2}, \tag{10}$$

the infinite series can be summed into a finite expression:

$$2\sum_{n=1}^{\infty} g(t,nb,y) = \frac{t^2-y^2-4ty}{(y+t)^3} + \frac{2\pi}{b}\coth \pi\frac{y+t}{b} - \frac{(y+3t)\pi^2}{b^2}\operatorname{csch}^2 \pi\frac{y+t}{b} + \frac{4ty\pi^3}{b^3}\operatorname{csch}^2 \pi\frac{y+t}{b}\coth \pi\frac{y+t}{b} + \frac{1}{y-t} \times \left[1 - 2\pi\frac{y-t}{b}\coth \pi\frac{y-t}{b} + \pi^2\left(\frac{y-t}{b}\right)^2 \operatorname{csch}^2 \pi\frac{y-t}{b}\right]. \tag{11}$$

It is further convenient to represent the kernel function in the following form

$$g(t,0,y) + 2\sum_{n=1}^{\infty} g(t,nb,y) = \frac{\pi}{b} g_1\left(\frac{\pi t}{b}, \frac{\pi y}{b}\right), \tag{12}$$

where the function g_1 can be written as

$$g_1(t,y) = \frac{1}{t-y} + 2\coth(y+t) - (y+3t)\operatorname{csch}^2(y+t) + 4ty\operatorname{csch}^2(y+t)\coth(y+t) + \frac{1}{y-t} \times [1 - 2(y-t)\coth(y-t) + (y-t)^2\operatorname{csch}^2(y-t)]. \tag{13}$$

Because function $D(t)$ is singular at the crack tip, it is now convenient to introduce a new unknown function $C(t)$

$$D(t) = \left(\frac{a^2}{a^2 - t^2}\right)^{1/2} C(t) \tag{14}$$

which is a smooth function. Equation (6) is thus transformed into the following equivalent integral equation for the unknown function $C(t)$

$$\frac{\pi}{b}\int_0^a C(t)\left(\frac{a^2}{a^2 - t^2}\right)^{1/2} g_1\left(\frac{\pi t}{b}, \frac{\pi y}{b}\right) \mathrm{d}t = -f_t f\left(\frac{y}{d}\right), \quad 0 < y < a. \tag{15}$$

Once the unknown function is solved, the stress intensity factor can be calculated as

$$K = \lim_{y \to a^+} \sqrt{2\pi(y - a)}\sigma_x(0, y) = -\pi\sqrt{a\pi}C(a). \tag{16}$$

Since the first term of the expression of function g_1 is $1/(t - y)$, (15) is actually a Cauchy's singular integral equation. To solve it numerically, we first introduce in the interval $(0, a)$ new variables

$$s = t/a, \quad x = y/a, \quad C(as) = B(s). \tag{17}$$

Now the singular integral equation (15) can be written in the form

$$\frac{\pi a}{b}\int_0^1 \frac{B(s)}{(1 - s^2)^{1/2}} g_1\left(\frac{\pi as}{b}, \frac{\pi ax}{b}\right) \mathrm{d}s = -f_t f\left(\frac{ax}{d}\right), \quad 0 < x < 1. \tag{18}$$

Next, (15) is extended into the interval $(-1, 1)$ by an even continuation:

$$B(-s) = B(s) \quad 0 < s < 1. \tag{19}$$

In this way, (15) can be equivalently expressed as

$$\frac{1}{2}\int_{-1}^1 \frac{B(s)}{(1 - s^2)^{1/2}} \frac{\pi a}{b} g_1\left(\left|\frac{\pi as}{b}\right|, \frac{\pi ax}{b}\right) \mathrm{d}s = -f_t f\left(\frac{ax}{d}\right), \quad 0 < x < 1. \tag{20}$$

A very accurate numerical solution can be obtained by Gauss–Chebyshev quadrature and the collocation technique as described by Erdogan et al. (e.g. [16] where n is replaced here by $2n + 1$), which converts the singular integral equation into a discrete form as

$$\begin{aligned} -f_t f\left(\frac{ax_j}{d}\right) &= \frac{1}{2}\sum_{i=1}^{2n+1} \frac{\pi}{2n+1} B(s_i) \frac{\pi a}{b} g_1\left(\left|\frac{\pi as_i}{b}\right|, \frac{\pi ax_j}{b}\right) \\ &= \sum_{i=1}^{n} \frac{\pi}{2n+1} B(s_i) \frac{\pi a}{b} g_1\left(\frac{\pi as_i}{b}, \frac{\pi ax_j}{b}\right), \quad j = 1, 2, \ldots, n, \end{aligned} \tag{21}$$

where n is the number of integration points. The unknown point coordinate s_i and the collocation point coordinate x_j are defined as

$$s_i = \cos\left(\frac{2i-1}{4n+2}\pi\right), \quad x_j = \cos\left(\frac{j\pi}{2n+1}\right). \tag{22}$$

Such a system of linear equations can be easily solved, for example, by the method of triangular factorization. Once we know B, we can calculate the stress intensity factor K in the form of the dimensionless stress intensity factor N as

$$N = \frac{K}{f_t\sqrt{2\pi b}} = -\frac{\pi\sqrt{a\pi}C(a)}{f_t\sqrt{2\pi b}} = -\frac{\pi}{f_t}\sqrt{\frac{a}{2b}}B(1). \tag{23}$$

Note that the numerical solution does not yield directly $B(1)$. The closest data point on which the unknown function is defined is $s_1 = \cos(\pi/(4n+2))$. In theory, an extrapolation, for instance a quadratic extrapolation, is needed to find $B(1)$. However, when n is large enough (for instance, $n = 50$), the difference between $B(1)$ and $B(s_1)$ is in the third of fourth digit, and thus is negligible.

The stress intensity factor, either in the form of K or the dimensionless form N, is obviously a function of a/b and d/b as well as the initial strain profile $f(y/d)$. Our purpose in the next section will be to find the relation between these geometric characteristics.

In terms of the dimensionless stress intensity factor N, we can rewrite the last equation in (4) as

$$\int_0^{a/b} N^2\left(x, \frac{d}{b}\right) \mathrm{d}x = \frac{a}{b}N^2\left(\frac{a}{b}, \frac{d}{b}\right). \tag{24}$$

Note that this equation is purely geometric, that is, it is independent of the material properties. From this equation, we can establish a relationship, which turns out to be one-to-one, between a/b and d/b. Furthermore, let

$$l_0 = \frac{G_f E}{f_t^2}. \tag{25}$$

This frequently used material characteristic, which will be called the material length, is an important quantity in the analysis. All the lengths characterizing the geometry will be normalized with respect to l_0. The second equation of (4) can now be converted to the form

$$N^2\left(\frac{a}{b}, \frac{d}{b}\right) = \frac{l_0}{2\pi b} = \frac{1}{2\pi b^*}, \tag{26}$$

where $b^* = b/l_0$ is the dimensionless crack spacing. Also, the dimensionless crack length and loading depth can be defined as

$$a^* = \frac{a}{l_0} = \frac{a}{b}b^*, \quad d^* = \frac{d}{l_0} = \frac{d}{b}b^*. \tag{27}$$

In the calculations, the ratio d/b is given as an input. Then, using (24) we can solve for a/b. After a/b and d/b are known, the value of b^* is determined from (26). The dimensionless

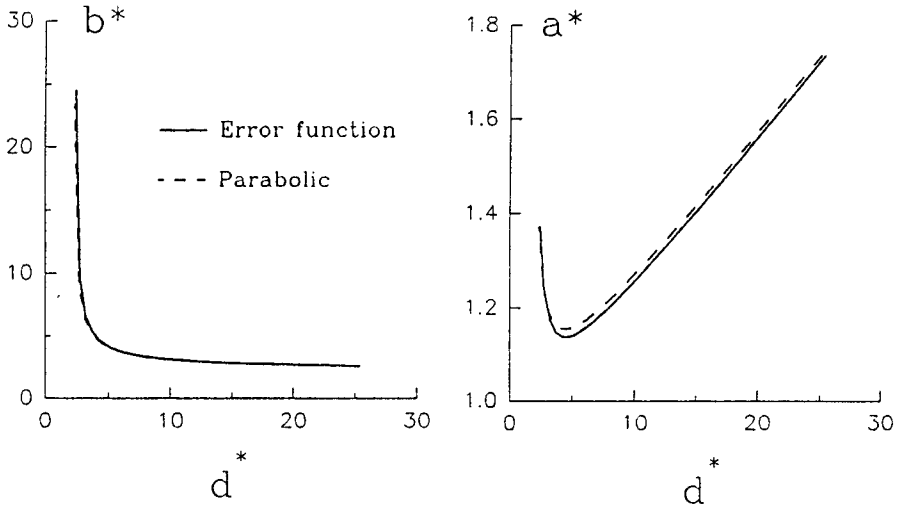

Fig. 2. (a) Crack spacing versus load depth; (b) Initial crack length versus load depth.

quantities a^* and d^* can be determined using (27). In this way, the problem can be solved efficiently.

4. Analysis of numerical results

Figure 2 shows the relation between a^* and d^*, as well as between b^* and d^*. The solid curve shows the error function and the dashed curve the parabolic function. As can be seen from Fig. 2, the difference in the final results between these two profiles is not significant. Thus, all the following analysis refers to the parabolic profile only. As the dimensionless loading depth d^* increases, the spacing b^*, starting from a very large value (which is actually infinite), decreases monotonically. However, the initial crack length first decreases. After it reaches its minimum value, it increases with d^* towards infinity. Such a behavior must reflect the requirement of energy balance. The crack driving force is controlled by the loading depth d^*. For small d^* there is only a small amount of energy available, and so the crack spacing must be very sparse, b^* must be very large and the crack length a^* must be very small. On the other hand, a larger d^* provides a larger amount of energy, and therefore a smaller crack spacing. Because the rate of decrease of b^* is initially dramatic, the energy available for each crack must be reduced. That is why the crack length must initially decrease with the loading depth. After the rate of decrease of b^* becomes less dramatic, the energy availability for each crack catches up, and then the crack length a^* begins to increase monotonically with d^*.

For very large d^*, the crack length a^* is also very large. Therefore, for the crack tip, the free surface at $y = 0$ is no longer important. In addition, when the loading depth increases without bounds, the initial strain distribution becomes uniform. The problem is thus transformed into an array of semi-infinite vertical cracks terminating at a common horizontal line subjected to a uniform pressure f_t acting horizontally at infinity. The stress intensity factor for this problem can be solved analytically using Fourier transformation [15], and the result is

$$K = f_t\sqrt{\tfrac{1}{2}b}. \tag{28}$$

Substituting this solution into the second equation of (4), we obtain the theoretical result for the lower limit of crack spacing $b^* = 2$. Such a limit serves as a check for our numerical

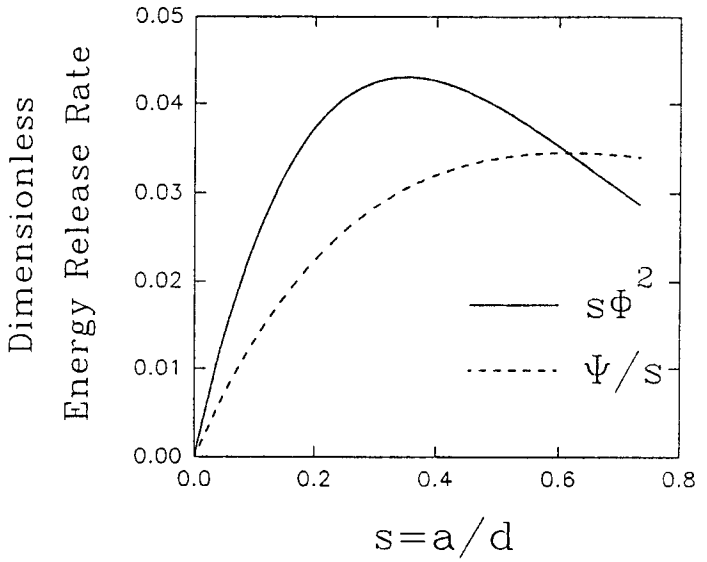

Fig. 3. Energy release rate and average energy release rate as function of a/d in the limiting case.

calculation. Specifying a large value of d/b, we can solve for b^*, which is found to be always larger, but very close to 2. For example, when $d^* = 100$, $b^* = 2.267$; when $d^* = 10^4$, $b^* = 2.026$. When $d^* = 10^5$, $b^* = 2.013$.

The other limit corresponds to a small d^* value when the spacing is infinitely large. Since the interaction between the cracks can be neglected, the problem can be transformed into a single crack in an elastic half-plane. The numerical method described in the previous section can certainly be modified to solve for the stress intensity factor for this configuration, but we prefer to use a simpler and more explicit approach. According to [15], the stress intensity factor can be expressed as

$$K = \frac{2f_t}{\sqrt{\pi a}} \int_0^a \frac{F(y/a)}{\sqrt{1-(y/a)^2}} f\left(\frac{y}{d}\right) \mathrm{d}y, \tag{29}$$

where $F(x) = 1.3 - 0.3x^{5/4}$. This formula has an error less than 0.5 percent. Inserting this equation into the second and the third conditions of crack initiation, we can transform these two equations into the dimensionless forms as

$$s\Phi^2(s) = \frac{\pi}{4d^*}, \quad \frac{\Psi(s)}{s} = \frac{\pi}{4d^*}, \tag{30}$$

where $s = a/d$ is a dimensionless variable, and the functions Φ and Ψ are defined as

$$\Phi(s) = \int_0^1 \frac{F(t)}{\sqrt{1-t^2}} f(st)\,\mathrm{d}t, \quad \Psi(s) = \int_0^s t\Phi^2(t)\,\mathrm{d}t. \tag{31}$$

To achieve adequate precision, Gauss–Chebyshev quadrature must be employed to calculate the function Φ. Combining the two equations in (30), we obtain an equation for determining the ratio a/d. Then, through either of the equations in (30), we can determine the value of

d^*. This value of d^* is found to be approximately 2.281, and the corresponding crack length $a^* = 1.411$ (when the initial strain profile is taken as a parabolic function). This result is also used as another check on our numerical calculations. The difference between the values just calculated and the extreme values of our previous numerical results is less than 0.4 percent.

The function $s\Phi^2(s)$ and $\Psi(s)/s$ is plotted in Fig. 3. Note that, away from the origin, there is only one point at which these two curves intersect. Such a point happens to be the maximum point of function $\Psi(s)/s$, which is the dimensionless form of the total energy released due to the crack formation. This property can easily be verified by the definition (30) of these two functions. The ratio $s = a/d = 0.6186$ is such that the total energy released is maximized among all the other ratios. As a result, the penetration depth is minimized.

One is naturally led to the question: what will happen when the maximum tensile stress exceeds the tensile strength of the material while the penetration depth d^* is still much less than the minimum value 2.281? Such a situation can happen, for instance, when the half plane represents a very hot object, the surface of which is suddenly brought into contact with a very cold medium. The surface stress quickly rises to $E\alpha(T_1 - T_0)$ (where α is the coefficient of thermal expansion and $T_1 - T_0$ is the temperature difference), but the penetration depth is initially very small because there is not enough time for the conduction of heat into the material.

According to this theory, when d^* is smaller than the lower limit value, there will not be enough stored energy available to create a crack, even though the stress level is already high enough to break the material. As a result, there will be densely distributed cracking which does not localize into cracks of macroscopic sizes. To avoid the trouble of smeared damage analysis, we assume that such behavior is approximately equivalent to the present analysis in which the maximum tensile stress can exceed the tensile strength, i.e.

$$\sigma_x(0, y) = \lambda f_t, \quad \lambda \geqslant 1. \tag{32}$$

When the stress condition is changed, the energy balance laws are also changed accordingly. In fact, the altered system will be the same as in (30), except that the dimensionless loading depth d^* must be replaced with $\lambda^2 d^*$. As a result, the critical ratio a/d is the same and the minimum penetration depth becomes $2.281/\lambda^2$, which is still finite, although smaller than the original minimum depth.

5. Experimental evidence

The present theory appears to be compatible with the existing experimental evidence. In Geyer's experiment [17], a glass plate uniformly heated to about 200°C was put into contact with dry ice (at −78°C). Seconds after contact, a few cracks suddenly shot up in a dynamic manner. Since the paper did not report what kind of glass was used in the test, we assume that it was soda-lime glass. For this kind of glass, the tensile strength is typically 70 MPa [1]. The typical standard deviation of the tensile strength of glass is about 20 percent. The Young's modulus reported in the paper is $E = 69$ GPa. The thermal expansion coefficient is 8.5×10^{-6} °C. The initial tensile stress caused by the temperature difference is calculated to be 160 MPa, which is larger than the tensile strength. If the fracture energy G_f is taken as 3.6 N/m, as reported in the paper, the material length l_0 is about 0.05 mm. With such a small reference length, only the part of the solution for small d^* and large b^* is relevant to this experiment.

It is observed that cracks do not form immediately after the hot glass gets in contact with dry ice. Rather, a few seconds are usually needed. This can be explained by our theory: the penetration depth needs to reach a certain length (a process that takes time) before the cracks can form. The average spacing is about 1 to 2 cm, which is sufficiently large for b^* to be regarded as infinity. In this experiment, the maximum stress is larger than the tensile strength (λ is about 2). An over-stressed plate can be highly unstable, since any disturbance supplying energy (such as kinetic energy) can make the energy sufficient for crack formation. If this occurs, the crack could form suddenly and in a dynamic manner. For dynamic crack growth another possible cause is the fact that the tensile strength of the glass decreases with an increase of temperature. Although the fracture energy also decreases with temperature, its rate of decrease is not as significant as that of the tensile strength. In the case of Geyer's test, the cold side of the glass plate is much stronger, therefore requires a higher level of stress to break the glass. However, once the cracks are formed and enter the zone of higher temperature, where the glass is less tough, then there is a surplus of crack driving force (that is, energy release rate). Such a surplus of driving force would certainly cause cracks to grow in a dynamic way.

6. Further considerations

It should be emphasized that the relation plotted in Fig. 2 between the penetration depth d^* and the crack spacing b^* (as well as the initial crack length a^*) does not apply for the subsequent crack evolution. Rather, each point in Fig. 2 represents an event of crack formation. After the cracks are formed, the dominant crack spacing is governed by the stability of the crack system and the bifurcation of solution. This has been discussed in detail in [3] [5] [2] and [12] [13].

Consider now the selection of d^*. Imagining that both the maximum value of the initial strain and the loading depth grow with time, one should take the loading depth at the moment when the maximum strain reaches the tensile strength. It is this loading depth that determines the initial crack spacing and the initial crack length. However, if the loading depth is still smaller than the minimum value, then the critical penetration depth will be the depth that first satisfies the relation $d^* = 2.281/\lambda^2$.

Nemat-Nasser et al. [12] gave an estimate of the lower limit of crack spacing, which is, using our notation, in the form of $b^* > 1/(\lambda^2 K_0)$; K_0 is an empirical coefficient depending on the initial strain loading profile, the ratio a/d and parameter θ representing the fraction of strain energy to be used in creating new crack surfaces. However, neither a/d nor θ can be determined in their analysis, as is admitted by Nemat-Nasser et al. [13]. In Geyer's paper, this factor is taken as 0.1. Therefore, their estimate of lower limit is 5 times larger than here.

Bažant et al. [5] gave a similar estimate. Their value of a/d was 1.5 or more, which is also larger than our result $a/d = 0.62$ (see Fig. 3). Further experimental studies are needed to verify these theoretical predictions.

According to the present analysis, the crack spacing has a lower bound, which is $d^* = 2$. For quasibrittle materials, the concept of fracture energy can no longer be uniquely defined, and different methods of fracture energy calibration suit different purposes. For concrete, the fracture energy obtained by the work-of-fracture method [18] is a measure of the energy required to tear apart a unit area of the material, which is usually 2 to 3 times larger than that obtained by the methods based on maximum-load measurements. It is the value obtained by the work-of-fracture method that should be employed in the calculation of the material length

l_0. More detailed discussion will be published elsewhere. For normal concrete, l_0 is in the range of 15–30 cm. Thus, in massive concrete blocks, the average surface crack spacing due to shrinkage is predicted to be no less than 30–60 cm.

For small scale fracture of sea ice, l_0 can be taken in the range of 5–10 cm; therefore, the average surface crack spacing due to temperature change in very thick sea ice plates should not be expected to be less than 10–20 cm.

According to the present type of theory, the length of the initial cracks in a finite body would have to depend also on the characteristic dimension (or size) of the structure, e.g. the thickness of a sea ice plate. Therefore, the crack initiation is a source of size effect. This has already been documented for the problem of initiation of radial cracks during the penetration of sea ice plate [11].

A comment on the limitation of the present theory is in order. Short enough cracks in all materials exhibit the so-called R-curve behavior which requires the use of some form of nonlinear fracture mechanics. The energy release rate of a very short crack (before reaching its final stage) is very small. Accordingly, our analysis implies the assumption that the crack will make a jump even though $G < G_f$ when crack length is very short. However, considering R-curve behavior, we realize that the initial crack growth may need less energy than G_f. Thus, the incremental energy balance equation could always be satisfied. These questions cannot be decided at present because the R-curve behavior has so far been documented only for short cracks starting from a notch, but not for cracks from a smooth surface. For those, the R-curve could be very different.

The most severe assumption probably is that of simultaneous occurrence of all the cracks. In real materials, the strength varies from point to point, and so cracks will start where the material is the weakest. Such cracks might not lose their stability due to R-curve behavior. As a result, more cracks could emerge. When the growing system of these small cracks loses its stability, only some of these small cracks, most likely those of longer lengths, will jump forward to their final stable positions. The assumption of our analysis could be approached if the material is very uniform, so the initial cracking is forced to occur nearly at the same time.

In this perspective, we realize that the true behavior of cracks at initiation is more complex than described in the form of the three conditions introduced in this paper. The possibility of an initial stable stage has been ignored, and so has been the perturbation due to the random inhomogeneity of the material. In addition, the nonlinear behavior described by damage mechanics is not taken into account, either. Consequently, the predictions of the present analysis are only approximations. However, the present analysis captures the basic aspects of the problem according to fracture mechanics and the stability point of view.

7. Conclusions

1. The initial spacing and initial stable equilibrium length of parallel equidistant cracks emanating from the surface of a half space can be determined from three conditions: (1) The stress at the surface reaches a given strength limit. (2) After the initial cracks form, the energy release rate equals its given critical value. (3) The finite energy release due to the initial crack jump equals the energy needed to form the crack (according to the given fracture energy of the material or fracture toughness).

2. The problem can be solved if the stress intensity factor as a function of the loading depth, the crack length and the crack spacing is known. The stress intensity factor can be

solved from a Cauchy integral equation. For the limiting cases of infinite initial crack length and of infinite large crack spacing, the correct limiting values are approached, which provides a check for the accuracy of the numerical solutions.

3. The results of analysis are compatible with the available experimental evidence on thermal cracks in glass. They also seem to agree with the experience for thermal cracks in sea ice and drying shrinkage cracks in concrete. However, further experimental verifications are needed.

Acknowledgment

Partial financial support under ONR grant N00014-91-J-1109 to Northwestern University (monitored by Dr. Yapa Rajapakse) is gratefully acknowledged. Additional support for studying the implications for concrete has been obtained from the Center for Advanced Cement-Based Materials at Northwestern University. Thanks are also due to Mr. Zheng Zhi Li for many hours of very stimulating discussion, which helped in understanding the limitation of the present analysis.

References

1. N.P. Bansal and P.H. Doremus, *Handbook of Glass Properties*, Academic Press, New York (1987).
2. Z.P. Bažant and L. Cedolin, *Stability of Structures: Elastic, Inelastic, Fracture and Damage Theories*, Oxford University Press, New York (1991).
3. Z.P. Bažant and H. Ohtsubo, *Mechanics Research Communications* 4 (1977) 353–366.
4. Z.P. Bažant and H. Ohtsubo, *International Journal for Numerical and Analytical Method in Geomechanics* 2 (1978) 317–327.
5. Z.P. Bažant, H. Ohtsubo, and K. Aoh, *International Journal of Fracture* 15 (1979) 443–456.
6. Z.P. Bažant and A.B. Wahab, *International Journal of Solids and Structures* 16 (1980) 97–106.
7. E.G. Frankenstein, *Load test data for lake ice sheet*, Technical Report 89, US Army Cold Region Research and Engineering Laboratory, Hanover, New Hampshire (1963).
8. I.S. Gradshteyn and I.M. Rhyzhik, *Tables of Integrals, Series and Products*, Academic Press, New York (1965).
9. L.M. Keer and K. Chantaramungkorn, *Journal of Applied Mechanics* 42 (1975) 683–691.
10. A.H. Lachenbruch, *Journal of Geophysical Research* 66 (1961) 4273–4275.
11. Y.N. Li and Z.P. Bažant, *Journal of Engineering Mechanics* 120 (1994) 1481–1498.
12. S. Nemat-Nasser, L.M. Keer, and K.S. Parihar, *International Journal of Solids and Structures* 14 (1978) 409–430.
13. S. Nemat-Nasser and A. Oranratnachai, *Journal of Energy Resources Technology* 101 (1979) 34–40.
14. H.F. Nied, *Journal of Applied Mechanics* 54 (1987) 642–648.
15. H. Tada, P. Paris, and G. Irwin, *The Stress Analysis of Cracks Handbook*, Del Research Corporation (1985).
16. F. Erdogan, G.D. Gupta and T.S. Cook, in *Methods of Analysis and Solutions of Crack Problems*, Noordhoff, Leyden (1973) 368–425.
17. J.F. Geyer and S. Nemat-Nasser, *International Journal of Solids and Structure* 18 (1982) 349–356.
18. A. Hillerborg, M. Modéer and P-E. Petersson, *Cement and Concrete Research* 6 (1976) 773–782.